Meteorology and Ozone, Temperature, Relative Humidity

J. Coates[1] and T. Butler[1]

[1]Institute for Advanced Sustainability Studies, Potsdam, Germany

November 27, 2015

Abstract

1 Introduction

Surface-level ozone (O_3) is a secondary air pollutant formed from the photochemical degradation of volatile organic compounds (VOCs) in the presence of nitrogen oxides (NO_x). Due to the photochemical nature of ozone production, meteorological factors such as temperature strongly influence ozone production (Jacob and Winner, 2009). Temperature influences ozone production through temperature-dependent emissions of VOC from biogenic sources (anthropogenic emissions are typically not temperature dependent) and the reaction rates of many of the chemical reactions involved in producing ozone are also temperature dependent. The recent review of Pusede et al. (2015) provides a detailed description of the temperature-dependent processes impacting ozone production. A recent study by indicates that temperature is a major meteorological driver for ozone in central europe.

Noelia's paper

Many studies over the US (Sillman and Samson, 1995; Dawson et al., 2007; Pusede et al., 2014) have observed the relationship between ozone and temperature, noting that increased temperatures tend to lead to higher ozone levels, often exceeding local air quality guidelines. Some of these studies (Sillman and Samson, 1995; Dawson et al., 2007) include modelling experiments using regional chemical tranport models which have indeed verified the observed increases in ozone with temperature. The increase in the thermal decomposition rate of PAN (peroxy acetyl nitrate) with temperature is commonly cited for the increase of ozone with temperature.

Environmental chamber studies have looked at the relationship of ozone with temperature using a particular mixture of VOCs. The chamber experiments of Carter et al. (1979) and Hatakeyama et al. (1991), also showed inreases in ozone with temperature and have also linked this relationship to increased PAN decomposition at higher temperatures (T >303 K). Hatakeyama et al. (1991) looked primarily at the influence of HO_2NO_2 decomposition on ozone production and induced that at lower temperatures (T < 303 K) HO_2NO_2 decomposition has a large influence on ozone production but the influence of PAN decomposition on ozone production increases with temperature.

Pusede et al. (2014) used observations over the San Joaquin Valley, California to infer a non-linear relationship of ozone production with temperature and NO_x, similar to the well-known non-linear relationship of ozone production on NO_x and VOC levels (Sillman, 1999). In fact, Pusede et al. (2014) show that temperature can be used as a surrogate for VOC levels when looking at the relationship of ozone across NO_x gradients. Moreover, the described relationship of ozone on both NO_x and temperature needs to be considered when looking at effective stratgies to reduce levels of surface ozone.

Despite a wealth of studies looking at the effects of temperature on ozone chemistry, there have not been (to our knowledge) modelling studies focusing on these effects across different NO_x gradients and whether the observed relationships are well-represented by different chemical mechanisms used in air quality models. The review of Pusede et al. (2015) also highlights a lack of modelling studies looking at this non-linear relationship of ozone on temperature across NO_x gradients. In this study, we use an idealised box model to determine how ozone levels vary with temperature and across NO_x gradients. We separate the effects of temperature-dependent chemistry and VOC emissions on ozone production by performing simulations including a temperature-independent source of isoprene followed by simulations using a temperature-dependent source of isoprene.

The study of Rasmussen et al. (2013) looking at the change of ozone with temperature in California (termed the "Ozone-Climate Penalty") indicates that changing the chemical mechanism used by a model may also change the Ozone-Climate Penalty and should be investigated. Finally, by repeating these simulations with different chemical mechanisms, we determine whether the temperature dependence of ozone production is reproduced across different NO_x gradients in these chemical mechanisms.

2 Methodology

2.1 Model Setup

- MECCA box model as described in Coates and Butler (2015) to broadly simulate the Benelux (Belgium, Netherlands and Luxembourg) region. As photolysis rates are parameterised by the solar zenith angle, the solar zenith angle of 51°N was used, representative of the central Benelux region.

- MECCA box model has been updated to include vertical mixing with the free troposphere and accordingly includes a diurnal cycle for the PBL height. These amendments are discussed further in Sect. 2.4.

- Simulations start at 06:00 using spring equinoctical conditions and the simulations ended after two days.

- All simulations performed using the Master Chemical Mechanism, MCM v3.2, (Rickard et al., 2015), Common Representative Intermediates, CRI v2 (Jenkin et al., 2008), Model for Ozone and related chemical tracers, MOZART-4 (Emmons et al., 2010), Regional Acid Deposition Model, RADM2 (Stockwell et al., 1990) and the Carbon Bond Mechanism, CB05 (Yarwood et al., 2005). Coates and Butler (2015) describes the implementation of these chemical mechanisms for use with KPP within MECCA. These chemical mechanisms were chosen as they are commonly used by modelling groups and represent the highly-detailed chemistry (MCM v3.2), chemistry suitable for regional 3D models (CRI v2, RADM2 and CB05) and global 3D models (MOZART-4).

- NOx emissions and temperature were varied systematically to analyse the effects on ozone mixing ratios over different NOx gradients at each temperature.

- VOC emissions constant until noon of first day, to simulate a plume of emitted VOC.

- Two sets of runs were performed – to include both a temperature-dependent and temperature-independent source of biogenic VOC emissions. MEGANv2.1 (Guenther et al., 2012) was used to specify the temperature-dependent BVOC emissions of isoprene. Isoprene is the most important VOC at a global scale due its high emission rates and emissions from vegetation have been reported to depend on temperature (Guenther et al.,

2006). In reality, increased temperature can also increase AVOC emissions by increasing evaporation of NMVOCs, this is not included in our study.

- Methane is fixed at 1.7 ppmv throughout the model run, carbon monoxide (CO) and ozone were initialised at 200 ppbv and 40 ppbv and then allowed to evolve freely throughout the the simulation.

- The temperature was systematically varied between 288 and 313 K (15 – 40 °C). The only source of NOx emissions in the box model was a constant source of NO emissions. The NO emissions were systematically varied from 5.0×10^9 to 1.5×10^{12} molecules (NO) cm^{-2} s^{-1} at each temperature used in this study.

2.2 VOC Emissions

- Anthropogenic emissions from Benelux for the year 2011 were obtained from the TNO-MACC_III emission inventory. TNO-MACC_III is the current version of the TNO-MACC_II inventory and was created using the same methodology as Kuenen et al. (2014) and based upon improvements to the existing emission inventory during the AQMEII-2 exercies described in Pouliot et al. (2015).

- Temperature-independent emissions of the biogenic VOC isoprene and monoterpenes, were calculated as a fraction of the total anthropogenic VOC emissions from each country in the Benelux region, this data was obtained from the supplementary data available from the EMEP (European Monitoring and Evaluation Programme) model (Simpson et al., 2012).

- AVOC and BVOC emissions are included as total emissions from SNAP (Selected Nomenclature for Air Pollution) source categories and these emissions were assigned to chemical groupings based on the country specific profiles for Belgium, the Netherlands and Luxembourg provided by TNO.

- The MCM v3.2 initial species were determined using the country specific profiles for each SNAP source category and where appropriate information of individual chemical species that can be represented by MCM v3.2 were determined using the detailed speciations of Passant (2002). This approach was also used in von Schneidemesser et al. (2015) and further details are found within this article.

Table 1: Total anthropogenic NMVOC emissions in 2011 in tonnes from each SNAP category assigned from TNO-MACC_III emission inventory and biogenic VOC emission in tonnes from Benelux region assigned from EMEP. The allocation of these emissions to MCM v3.2, CRI v2, CB05, MOZART-4 and RADM2 species is found in the supplement.

	SNAP1	**SNAP2**	**SNAP34**	**SNAP5**	**SNAP6**	**SNAP71**
Belgium	4494	9034	22152	5448	42809	6592
Netherlands	9140	12173	29177	8723	53535	16589
Luxembourg	121	44	208	1371	4482	1740
Total	13755	21251	62648	15542	100826	24921
	SNAP72	**SNAP73**	**SNAP74**	**SNAP8**	**SNAP9**	**BVOC**
Belgium	2446	144	210	6448	821	7042
Netherlands	3230	1283	1793	10067	521	1462
Luxembourg	1051	6	324	643	0	2198
Total	6727	1433	2327	17158	1342	10702

- As in von Schneidemesser et al. (2015), first the primary VOC that are represented by the MCM v3.2 and respective emissions were determined. Using this MCM v3.2 data, the NMVOC emission data were mapped to mechanism species in the other four chemical mechanisms used in the study. The NMVOC emissions in the non-MCM v3.2 chemical mechanisms were weighted by the carbon numbers of the MCM v3.2 species and the emitted mechanism species. The supplementary data outlines the primary NMVOC and calculated emissions with each chemical mechanism.

2.3 Temperature Dependent Isoprene Emissions

- Temperature dependent isoprene emissions were estimated using the MEGAN2.1 algorithm (Guenther et al., 2012).
- The aim of the study is to look at the effects of temperature, hence in the MEGAN2.1 algorithm all parameters (except temperature) were kept constant.
- The boxmodel setup uses a constant temperature throughout the model run and so the parameters T_{24} and T_{240}, the average temperatures in the past 24 and 250 hours, were assumed to be constant and equal to the temperature value of the boxmodel.
- Constant PAR (photosynthetically active radiation) and LAI (leaf area index) were used at each temperature step.
- The LAI, plant functional type (PFT) and associated isoprene emission factor were taken from Guenther et al. (2012) and selected to give the same isoprene mixing ratios at a temperature of 293 K as in the temperature independent modelling case. For all other model runs over the different temperature, the MEGAN2.1 algorithm was used to estimate the isoprene emissions.
- Thus using this idealised case, we can determine the effects of increasing isoprene emissions with temperature across NO_x gradients.
- This was repeated for each chemical mechanism.
- As in the temperature independent model runs, the emissions of NMVOC and the temperature dependent source of isoprene, were held constant until noon of the first day.
- Using these assumptions, the isoprene emissions at each temperature step of the study are illustrated in Fig. 1 and show the expected exponential increase in emissions with temperature (Guenther et al., 2006).

2.4 Vertical Mixing with Diurnal Boundary Layer Height

- The MECCA box model used in Coates and Butler (2015) included a constant boundary layer height of 1 km and no interactions (vertical mixing) with the free troposphere.

Figure 1: The estimated isoprene emissions (molecules isoprene cm^{-2} s^{-1}) at each temperature step used in the study. Isoprene emissions were estimated using the MEGAN2.1 algorithm (Guenther et al., 2012).

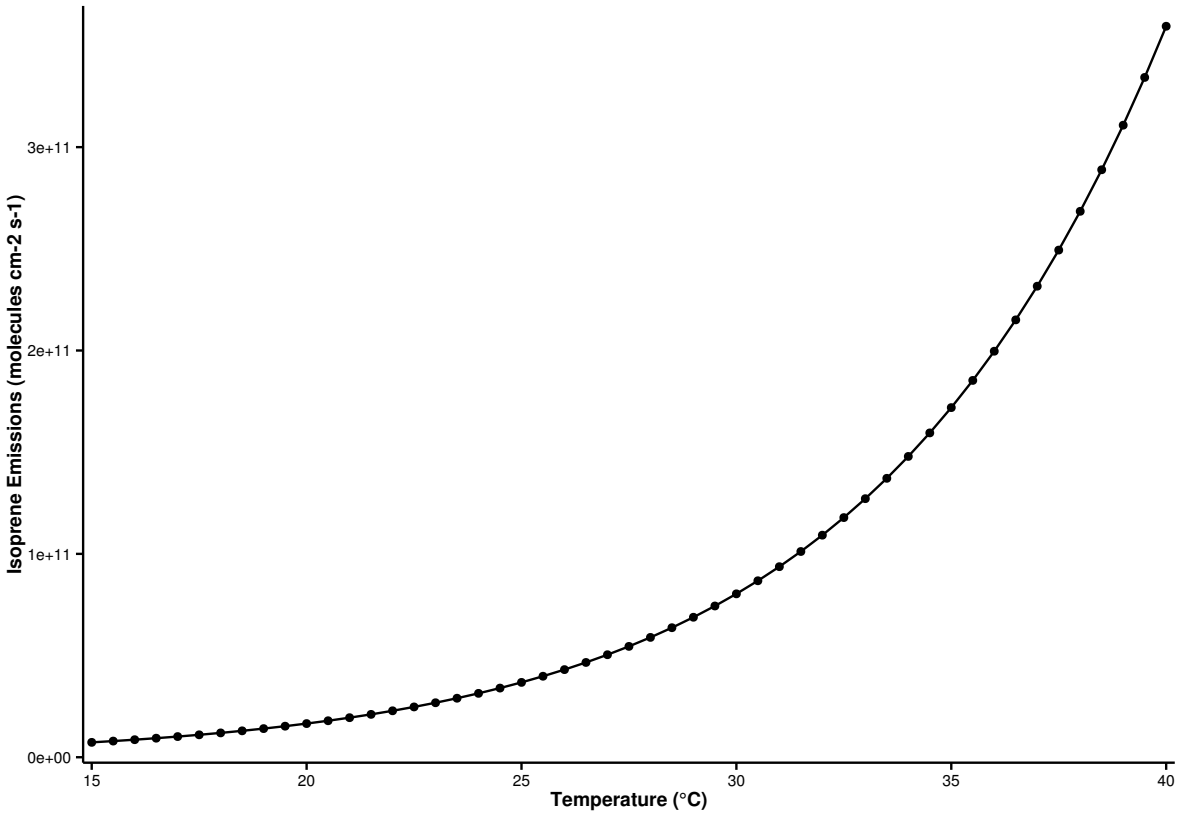

- The planetary boundary layer (PBL) height varies diurnally and affects chemistry by diluting emissions after sunrise when the PBL rises. The expansion of the PBL into the free troposphere introduces vertical mixing with those chemical species present in the free troposphere. When the PBL collapses in the evening, pollutants are trapped in the PBL.

- The mixing layer height was measured as part of the BAERLIN campaign over the city of Berlin, Germany. The profile of mean mixing layer height during the campaign period (June – August 2014) was used in the model to represent the diurnal cycle of the mixing layer height.

Reference Boris' paper

- The concentrations of the chemical species within the PBL are diluted due to the larger mixing volume when the PBL height increases at the beginning of the day, also the increasing PBL height mixes the chemical species from the free troposphere with the chemical species within the PBL i.e. vertical mixing. The PBL height collapses during night leaving the stable nocturnal boundary layer, trapping the chemical species into a smaller volume thus increasing the concentrations of the chemical species.

- This vertical mixing scheme was implemented into the boxmodel using the same approach of Lourens (2012).

- The mixing ratios of O3, CO and CH4 in the free troposphere were respectively set to 50 ppbv, 116 ppbv and 1.8 ppmv. These conditions were taken from the MATCH-MPIC chemical weather forecast model on the 21st March (the start date of the simulations). The model results (`http://cwf.iass-potsdam.de/`) at the 700 hPa height were chosen and the daily average was used as input into the boxmodel.

check reference

3 Results

3.1 Ozone mixing ratios as function of NOx and Temperature

Figure 2 depicts the maximum mixing ratio of ozone obtained from each model run as a function of the total NO_x emissions on the first day and temperature. Using each mechanism, a similar non-linear relationship of ozone mixing ratios on NO_x and temperature is found and increased ozone levels are found at higher temperatures when including a temperature-dependent source of isoprene emissions. CB05 and RADM2 produce the largest amount of ozone at higher temperatures and higher NO_x levels than the other chemical mechanisms.

Figure 2: Contours of maximum ozone mixing ratio as a function of the total NO_x emissions on the first day and daily temperature for each chemical mechanism and using both a temperature-dependent and -independent source of isoprene emissions.

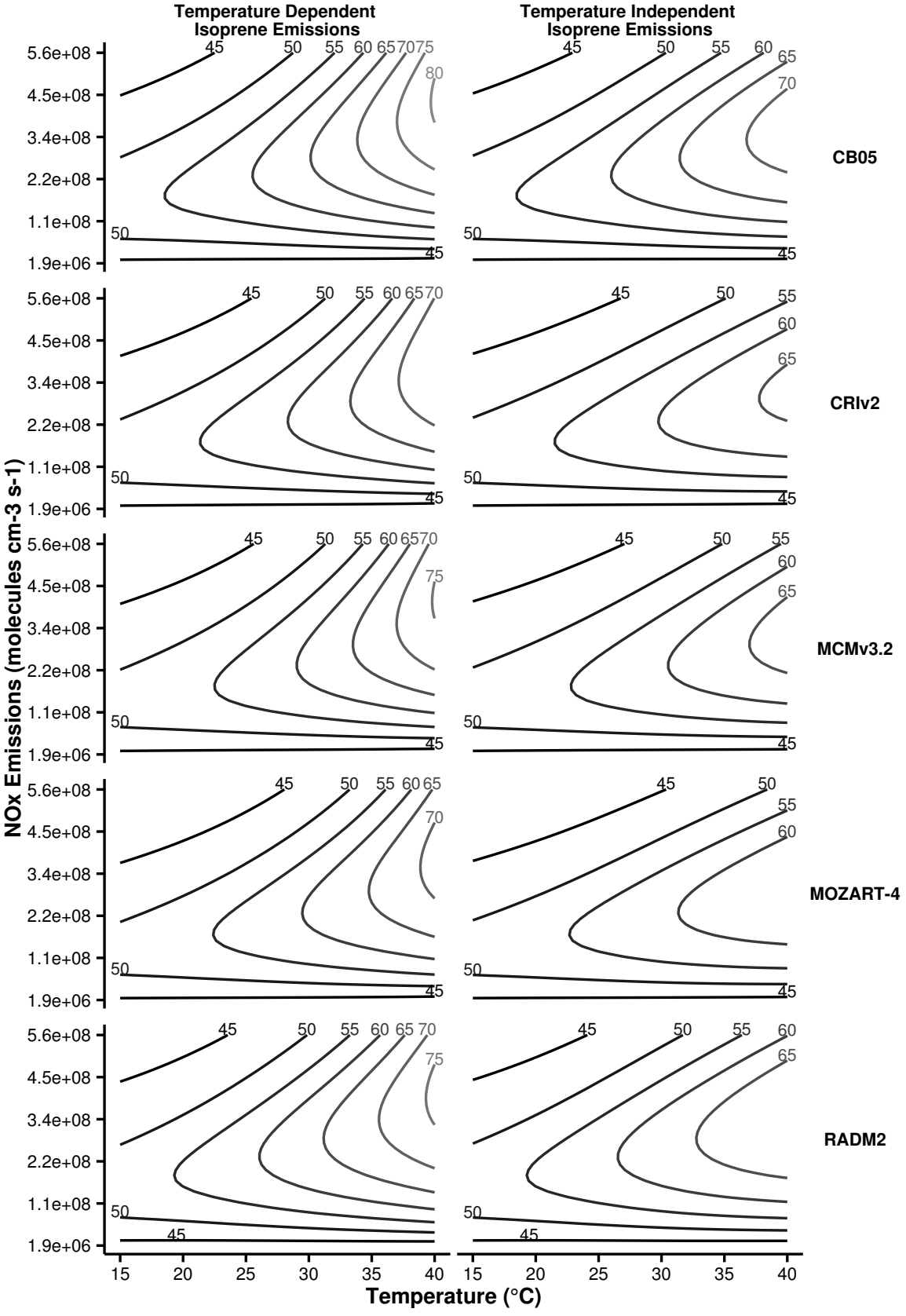

Table 2: Percentage increase in ozone mixing ratios at maximum temperature (40 °C) from reference temperature (20 °C) in Temperature Dependent and Independent Experiments.

Mechanism	Run	High-NO_x	Maximal-O_3	Low-NO_x
MCMv3.2	TI	31 %	24 %	14 %
	TD	53 %	38 %	23 %
	TD - TI	22 %	14 %	9 %
CRIv2	TI	28 %	21 %	12 %
	TD	50 %	36 %	22 %
	TD - TI	22 %	15 %	10 %
MOZART-4	TI	26 %	19 %	12 %
	TD	47 %	32 %	21 %
	TD - TI	21 %	13 %	9 %
CB05	TI	40 %	29 %	19 %
	TD	59 %	42 %	28 %
	TD - TI	19 %	13 %	9 %
RADM2	TI	35 %	26 %	17 %
	TD	50 %	36 %	25 %
	TD - TI	15 %	10 %	8 %

The temperature-dependent source of isoprene leads to increased ozone mixing ratios at higher temperatures and higher NO_x levels (top-right of each plot in Fig. 2). The largest increase in ozone is found in the MCMv3.2 and CRIv2, where the ozone increased by 16 ppbv when using temperature-dependent isoprene emissions. All other mechanisms, had similar increases in ozone with temperature-dependent isoprene emissions; RADM2 with an increase of 11 ppbv had the lowest increase in ozone. At low temperatures, regardless of the NO_x level, similar amounts of ozone are predicted from both the temperature-dependent and temperature-independent sources of isoprene emissions.

3.2 Ozone budgets

We defined the O_x family to consist of

complete this and reasons

Sillman (1995) shows that the ratio of HNO_3 to H_2O_2 can be used to determine whether an atmospheric system is in a NO_x-sensitive, VOC-sensitive or in the ridge region of the NO_x-VOC relationship with ozone, where maximum ozone is produced. Based on this, we assigned each model run used to generate the ozone contours in Fig. 2 to three NO_x regimes–Low-NOx, High-NOx and Maximal-O3–corresponding to NO_x-sensitive, VOC-sensitive and NO_x-VOC-sensitive regions defined by Sillman (1995). Values of H_2O_2/HNO_3 less than 0.3 correspond to the High-NOx regime, values larger than 0.5 correspond to the Low-NOx regime and all values inbetween correspond to the ridge area in which maximal ozone is produced.

In Fig. 3, the production rates on the first day of each reaction contributing to the

Figure 3: The contributions of the different reactions to total O_x budget at each temperature at different NO_x levels.

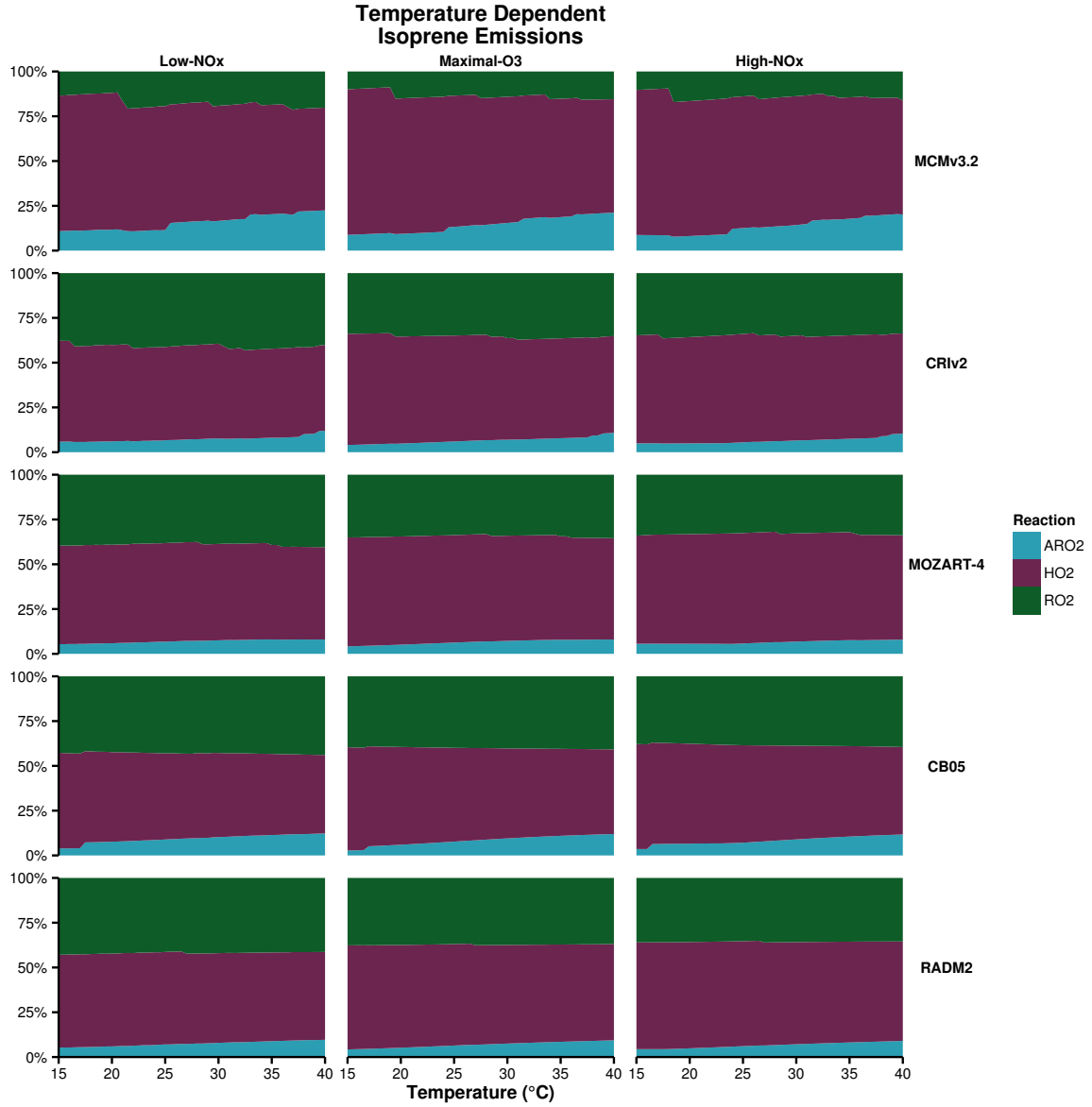

Figure 4: Correlation of mean ozone mixing ratio with temperature in Low-NOx, maximal-O3 and High-NOx conditions for each chemical mechanism. A linear relationship between mean ozone mixing ratios and temperature is inferred, regression statistics are found in Table 3.

Table 3: Regression statistics for the linear relationship between ozone mixing ratios and temperature shown in Figure 4.

Mechanism	**NOx Condition**	**Temperature Dependent Isoprene Emissions**		**Temperature Independent Isoprene Emissions**	
		Slope ($m_{O3\text{-}T}$)	**R^2**	**Slope ($m_{O3\text{-}T}$)**	**R^2**
CB05	Low-NOx	0.6	0.95	0.4	0.98
	Maximal-O3	1.0	0.96	0.8	0.99
	High-NOx	1.3	0.94	0.9	0.97
CRIv2	Low-NOx	0.4	0.94	0.3	0.99
	Maximal-O3	0.8	0.96	0.5	0.99
	High-NOx	1.0	0.93	0.6	0.98
MCMv3.2	Low-NOx	0.5	0.93	0.3	0.98
	Maximal-O3	0.8	0.95	0.6	0.98
	High-NOx	1.0	0.92	0.7	0.97
MOZART-4	Low-NOx	0.4	0.96	0.3	0.99
	Maximal-O3	0.7	0.97	0.5	1.00
	High-NOx	0.9	0.93	0.6	0.98
RADM2	Low-NOx	0.5	0.97	0.4	0.99
	Maximal-O3	0.9	0.98	0.7	1.00
	High-NOx	1.1	0.95	0.8	0.98

O_x production budget are determined and these reaction rates are then averaged over each NO_x-condition (Low-NO_x, High-NO_x and Maximal-O3). The fractional contribution of this reaction rate to the total O_x budget was then calculated for each NO_x-condition.

Figure 3 shows that the reaction of the hydroperoxyl radical (HO_2) with NO has the largest contribution at each NO_x-condition, but this fractional contribution decreaes at higher temperatures due to the increased contributions of other reactions. The increased contribution of the reaction of the acetyl peroxy radical (CH_3CO_3) with NO with temperature has the most significant contribution to the total O_x budget and this contribution is higher in CB05 and RADM2 compared to the other chemical mechanisms.

Add quantitative values of differences.

3.3 Rate of Change of Ozone with Temperature

Each model run was allocated the three NO_x-conditions as described in Sect. 3.2 and then the mean ozone mixing ratio in these NO_x regimes were then correlated with temperature as shown in Fig. 4. In literature, a linear relationship is typically reported between ozone and temperature and so the linear regression statistics are reported in Table 3.

The linear increase of ozone with temperature, $m_{O3\text{-}T}$ in Table 3, is highest at high-NOx conditions for each chemical mechanism and for each temperature case of isoprene emissions. The high-NOx regime corresponds to the top regions of the contour plots in Fig. 2 where increases in temperature would shift the ozone production towards the ridge of maximal ozone production, thus this increase in $m_{O3\text{-}T}$ is expected. Similarly, the lowest $m_{O3\text{-}T}$ are achieved in the low-NOx regime, the bottom regions of the contours in Fig. 2, where increases in temperature do not neccisarily lead to increased ozone levels.

4 Discussion

4.1 Ozone Contours

The ozone contours of Fig.2 illustrate the non-linear relationship of ozone mixing ratios to NO_x and temperature which is similar to the contours of ozone production to NO_x mixing ratios and temperature demonstrated in Pusede et al. (2014). The relationship determined in Pusede et al. (2014) is relevant to the San Joaquin Valley, California and was inferred using observational methods.

As highlighted by the review of Pusede et al. (2015) the dependence of ozone to temperature is multi-faceted and is influenced by increased emissions, in particular BVOC such as isoprene emitted from biogenic species, and increased rates of chemical reactions. The increase in isoprene emissions with temperature is shown to be the more important than the increase of ozone production chemistry through increased reaction rates in Fig. 2, as here there is a large increase in ozone at higher temperatures with increased isoprene emissions alone rather than the increased chemistry.

In order to determine how important the effect of increasing isoprene emissions with temperature are in relation to increases in ozone production chemistry, we repeated the sets of model runs at each NO_x condition and temperature using a constant source of isoprene equal to that emitted at the lowest temperature (288 K) and then the highest temperature (313 K). The

results of these model runs show that ...

The increase in ozone with temperature tends to follow the same shape as the increase of isoprene emissions with temperature (Fig. 1), showing that the increase of isoprene emissions with temperature may be the dominant factor of increased ozone with temperature.

4.2 Ozone Budgets

The reaction of CH_3CO_3 with NO has the highest contribution to the total O_x budget at higher temperatures in each NO_x condition in Fig. 3. The main source of CH_3CO_3 is its chemical equilibrium with PAN, in the presence of NO_2, other than this equilibrium it is the degradation of acetaldehyde (CH_3CHO) that leads to a net source of CH_3CO_3.

The increased contribution of CH_3CO_3 reaction with NO to O_x production budget is more pronounced in the CB05 and RADM2 chemical mechanisms. Acetaldehyde is included in the NMVOC emissions of each chemical mechanism, however it also has a chemical source from the secondary degradation on many other NMVOC. An increased chemical source of CH_3CHO from the representation of tropospheric degradation chemistry in CB05 and RADM2 could be the cause of the higher ozone mixing ratios when using CB05 and RADM2 chemical mechanisms.

Coates and Butler (2015) have shown that the secondary degradation of the RADM2 species HC3 under-estimates the yields of less-reactive ketones at the expense of increased aldehyde yields. Thus the increased aldehyde yields propagate ozone production through the reactions of the degradation products CH_3CO_3 and the methyl peroxy radical (CH_3O_2) with NO. Moreover, in the CB05, the are no ketone species present in this chemical mechanism and the chemical source of carbonyl species is mainly in the form of aldehydes, leading to a similar propagation of ozone production as described for RADM2. Thus the underestimation or missing representation of the yield of ketone species in the RADM2 and CB05 chemical mechanisms leads to higher ozone production and the larger ozone mixing ratios seen in Fig. 2.

The increased amounts of CH_3CO_3 simulated with RADM2 and CB05 also influences another well-known aspect of the relationship of ozone with temperature, namely that at higher temperatures peroxy nitrates (RO2NO2), such as PAN, are no longer a suitable reservoir of peroxy radicals and NO_x due to an increase in PAN decomposition rates with temperature, leading to re-release of peroxy radicals and NO_2 which can then go on to further produce ozone. As the chemistry of RADM2 and CB05 produces more CH_3CO_3 this leads to an increase in the mixing ratios of RO2NO2, mainly PAN in RADM2 and CB05, and so the equilibrium state is

shifted in these chemical mechanisms compared to the MCM v3.2, CRI v2 and MOZART-4. This shift in equilibrium state is another pathway for increased ozone production with temperature in the CB05 and RADM2.

4.3 Rate of Change of Ozone with Temperature

5 Conclusions

References

William P. L. Carter, Arthur M. Winer, Karen R. Darnall, and James N. Pitts Jr. Smog chamber studies of temperature effects in photochemical smog. *Environmental Science & Technology*, 13 (9):1094–1100, 1979.

J. Coates and T. M. Butler. A comparison of chemical mechanisms using tagged ozone production potential (TOPP) analysis. *Atmospheric Chemistry and Physics*, 15(15):8795–8808, 2015.

John P. Dawson, Peter J. Adams, and Spyros N. Pandis. Sensitivity of ozone to summertime climate in the eastern USA: A modeling case study . *Atmospheric Environment*, 41(7):1494 – 1511, 2007.

L. K. Emmons, S. Walters, P. G. Hess, J.-F. Lamarque, G. G. Pfister, D. Fillmore, C. Granier, A. Guenther, D. Kinnison, T. Laepple, J. Orlando, X. Tie, G. Tyndall, C. Wiedinmyer, S. L. Baughcum, and S. Kloster. Description and evaluation of the Model for Ozone and Related chemical Tracers, version 4 (MOZART-4). *Geoscientific Model Development*, 3(1):43–67, 2010.

A. Guenther, T. Karl, P. Harley, C. Wiedinmyer, P. I. Palmer, and C. Geron. Estimates of global terrestrial isoprene emissions using MEGAN (Model of Emissions of Gases and Aerosols from Nature). *Atmospheric Chemistry and Physics*, 6(11):3181–3210, 2006.

A. B. Guenther, X. Jiang, C. L. Heald, T. Sakulyanontvittaya, T. Duhl, L. K. Emmons, and X. Wang. The Model of Emissions of Gases and Aerosols from Nature version 2.1 (MEGAN2.1): an extended and updated framework for modeling biogenic emissions. *Geoscientific Model Development*, 5(6):1471–1492, 2012.

Shiro Hatakeyama, Hajime Akimoto, and Nobuaki Washida. Effect of temperature on the

formation of photochemical ozone in a propene-nitrogen oxide (NOx)-air-irradiation system. *Environmental Science & Technology*, 25(11):1884–1890, 1991.

Daniel J. Jacob and Darrell A. Winner. Effect of climate change on air quality. *Atmospheric Environment*, 43(1):51 – 63, 2009. Atmospheric Environment - Fifty Years of Endeavour.

M.E. Jenkin, L.A. Watson, S.R. Utembe, and D.E. Shallcross. A Common Representative Intermediates (CRI) mechanism for VOC degradation. Part 1: Gas phase mechanism development. *Atmospheric Environment*, 42(31):7185 – 7195, 2008.

J. J. P. Kuenen, A. J. H. Visschedijk, M. Jozwicka, and H. A. C. Denier van der Gon. TNO-MACC_II emission inventory; a multi-year (2003–2009) consistent high-resolution european emission inventory for air quality modelling. *Atmospheric Chemistry and Physics*, 14(20): 10963–10976, 2014.

AsM Lourens. *Air quality in the Johannesburg-Pretoria megacity: its regional influence and identification of parameters that could mitigate pollution.* PhD thesis, North-West University, Potchefstroom Campus, 2012.

N. Passant. Speciation of UK emissions of non-methane volatile organic compounds. Technical report, DEFRA, Oxon, UK., 2002.

George Pouliot, Hugo A.C. Denier van der Gon, Jeroen Kuenen, Junhua Zhang, Michael D. Moran, and Paul A. Makar. Analysis of the emission inventories and model-ready emission datasets of Europe and North America for phase 2 of the AQMEII project. *Atmospheric Environment*, 115: 345–360, 2015.

S. E. Pusede, D. R. Gentner, P. J. Wooldridge, E. C. Browne, A. W. Rollins, K.-E. Min, A. R. Russell, J. Thomas, L. Zhang, W. H. Brune, S. B. Henry, J. P. DiGangi, F. N. Keutsch, S. A. Harrold, J. A. Thornton, M. R. Beaver, J. M. St. Clair, P. O. Wennberg, J. Sanders, X. Ren, T. C. VandenBoer, M. Z. Markovic, A. Guha, R. Weber, A. H. Goldstein, and R. C. Cohen. On the temperature dependence of organic reactivity, nitrogen oxides, ozone production, and the impact of emission controls in San Joaquin Valley, California. *Atmospheric Chemistry and Physics*, 14(7):3373–3395, 2014.

Sally E. Pusede, Allison L. Steiner, and Ronald C. Cohen. Temperature and Recent Trends in the Chemistry of Continental Surface Ozone. *Chemical Reviews*, 115(10):3898–3918, 2015.

D. J. Rasmussen, Jianlin Hu, Abdullah Mahmud, and Michael J. Kleeman. The ozone–climate penalty: Past, present, and future. *Environmental Science & Technology*, 47(24):14258–14266, 2013. PMID: 24187951.

Andrew Rickard, Jenny Young, M. J. Pilling, M. E. Jenkin, Stephen Pascoe, and S. M. Saunders. The Master Chemical Mechanism Version MCM v3.2. `http://mcm.leeds.ac.uk/MCMv3.2/`, 2015. [Online; accessed 25-March-2015].

Sanford Sillman. The use of NOy, H2O2, and HNO3 as indicators for ozone-NOx-hydrocarbon sensitivity in urban locations. *Journal of Geophysical Research: Atmospheres*, 100(D7): 14175–14188, 1995.

Sanford Sillman. The relation between ozone, NOx and hydrocarbons in urban and polluted rural environments. *Atmospheric Environment*, 33(12):1821 – 1845, 1999.

Sanford Sillman and Perry J. Samson. Impact of temperature on oxidant photochemistry in urban, polluted rural and remote environments. *Journal of Geophysical Research: Atmospheres*, 100(D6):11497–11508, 1995.

D. Simpson, A. Benedictow, H. Berge, R. Bergström, L. D. Emberson, H. Fagerli, C. R. Flechard, G. D. Hayman, M. Gauss, J. E. Jonson, M. E. Jenkin, A. Nyíri, C. Richter, V. S. Semeena, S. Tsyro, J.-P. Tuovinen, Á. Valdebenito, and P. Wind. The EMEP MSC-W chemical transport model – technical description. *Atmospheric Chemistry and Physics*, 12(16):7825–7865, 2012.

William R. Stockwell, Paulette Middleton, Julius S. Chang, and Xiaoyan Tang. The second generation regional acid deposition model chemical mechanism for regional air quality modeling. *Journal of Geophysical Research: Atmospheres*, 95(D10):16343–16367, 1990.

E. von Schneidemesser, J. Coates, A. J. H. Visschedijk, H. A. C. Denier van der Gon, and T. M. Butler. Variation of the NMVOC speciation in the solvent sector and the sensitivity of modelled tropospheric ozone. *Atmospheric Environment*, page In preparation, 2015.

Greg Yarwood, Sunja Rao, Mark Yocke, and Gary Z. Whitten. Updates to the Carbon Bond Chemical Mechanism: CB05. Technical report, U. S Environmental Protection Agency, 2005.